A Pigment Precursor Based on 1,4-diketo-3,6-diphenyl-pyrrolo-[3,4-c]-pyrrole and its Regeneration into the Pigment

J. Mizuguchi✦
Graduate School of Engineering, Yokohama National University, Yokohama, JAPAN

The title compound is a soluble precursor ("latent pigment": *t*-BOC DPP) of diketopyrrolopyrrole pigment (DPP) that can be used for electronic and imaging applications in LCD color filters, ink jet and thermal printers. The regeneration and regenerated product of *t*-BOC DPP have been studied in terms of thermogravimetric and X-ray diffraction analyses, as well as IR and diffuse reflectance spectra on powdered substances. Transformation from *t*-BOC DPP to the parent DPP begins around 160°C and is completed around 180°C. A variety of colors (yellow via yellowish red to red) appear during the regeneration process, accompanied by evolution of CO_2. Further color change also occurs due to aging and dispersion in vehicles. The color as well as the structure of regenerated DPP is slightly different from that of commercial DPP, and the heat and light stability is again not as high as that of the commercial product.

Journal of Imaging Science and Technology 49: 35–40 (2005)

Introduction

Diketopyrrolopyrrole (DPP, Fig. 1) is a well known, red pigment on the market.[1] DPP is a small molecule and colored only pale yellow in solution, but it becomes vivid red in the solid state due to intermolecular interactions.[2] DPP is also stabilized due to the intermolecular hydrogen-bond network between the NH group of one molecule and the O atom of the neighboring one. Because of this, a cluster of small DPPs becomes a polymer-like substance.

The "latent pigment" of the title compound is a soluble, yellowish precursor of DPP developed by Zambounis, Hao and Iqbal at CIBA Specialty Chemicals.[3,4] The soluble precursor is prepared by replacing the H atom of the NH group with a *t*-butoxycarbonyl (*t*-BOC) group: the precursor is hereafter called *t*-BOC DPP. The insoluble parent DPP can then be regenerated by thermal decomposition of the precursor around 180°C (Fig. 1). The present latent pigments have been developed with a concept that unites the advantageous properties of a pigment and a dyestuff. Dyes readily dissolve in the application medium, offering several advantages over a pigment in terms of transparency, saturation and strength of coloration. On the other hand, pigments are insoluble and feature superior heat, light and chemical fastness. However, they are generally used as submicron particles dispersed in the application medium. To achieve this, it requires time and energy consuming milling, recrystallization and dispersion steps. Therefore, the present "latent pigment technology" is a versatile and promising technique for the preparation of nano pigment particles as well as transparent thin films for electronic applications such as LCD color filters (LCD: liquid crystal display).

The latent pigments also find potential applications to ink jet printing. The ink jet ink is prepared on the basis of the latent pigment and then deposited onto a substrate. After that, regeneration of the latent pigment is made directly on the substrate. In this way, we can obviate the clogging problem of pigment-based inks. It is also important to note that the latent pigment can easily be sublimed at temperatures lower than those required for regeneration. Therefore, three primary colors of latent pigments can be transferred onto a sheet of paper by a thermal head. Then, a full color picture appears at one regeneration. In order to achieve these, it is indispensable to study the regeneration process in detail in consideration of the regenerated color and its stability.

The first part of this paper describes briefly the crystal structure of two crystal modifications (α and β) of *t*-BOC DPP. Then, the second part deals with the regeneration process from *t*-BOC DPP to the parent DPP as well as the characterization of regenerated DPP. The crystal structure of DPP has previously been reported by us.[5] Regarding the structure of *t*-BOC DPP, MacLean and others reported that there exist two crystal modifications (α and β) and simulated the structure on the basis of powder X-ray diffraction diagrams.[6] On the other hand, we have recently carried out full structure analysis of these modifications on single crystals.[7,8]

Original manuscript received March 1, 2004

✦ IS&T Fellow

Corresponding Author: J. Mizuguchi, mizu-j@ynu.ac.jp

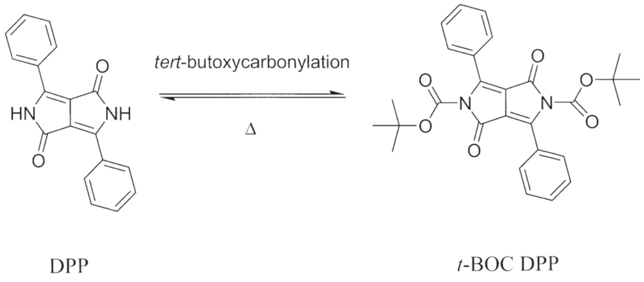

Figure 1. DPP and t-BOC DPP and the regeneration process.

Experimental

Preparation of Materials

t-BOC DPP was prepared according to the method previously reported in Ref. 3. The product obtained was of the β form (yellow); whereas the α form (yellowish orange) was obtained by dissolving the product in acetonitrile, followed by slow solvent evaporation. The β form was used for the present regeneration experiments, since no significant difference between the α and β forms is recognized in either TGA (thermogravimetric analysis) or diffuse reflectance spectra as shown below.

The t-BOC DPP sample used for IR measurements was directly prepared onto a KBr disk by means of spin coating, using a saturated dioxane solution. The sample was then used for successive measurements at various temperatures.

The parent DPP used for comparison with regenerated DPP was purchased from CIBA Specialty Chemicals Inc.

Equipment

Diffuse reflectance spectra for powdered pigments were measured on a UV-2400PC spectrophotometer together with an integrating sphere attachment (ISR-240A from Shimadzu). The diffuse reflectance spectra were corrected by the Kubelka–Munk equation. Thermo-gravimetric analysis (TGA) was made by a Rigaku Thermo Plus 8230 on powdered samples at a heating rate of 10°C/min. Powder X-ray diffraction diagrams were measured on a Rigaku Diffractometer (model: Rapid F).

Results and Discussion

Crystal Structures of the α and β Forms

Table I details the crystallographic parameters for the α and β modifications[7,8] together with those of the simulation based on powder diffraction data.[6] The crystal system is monoclinic for both α and β forms and the space group is $P2_1/n$, $P2_1/c$, respectively. The lattice parameters for the α form are in good agreement with those of the simulation, but some difference is still recognized in torsion angles. The α form crystallizes with one and half molecules (A and B) in the asymmetric unit. Molecule A resides on a general position of C_1 symmetry while molecule B is on a special position of C_i symmetry. All together, there are 6 molecules in the unit cell: four of molecule A and two of molecule B. On the other hand, in the β form, t-BOC DPP crystallizes in space group $P2_1/c$ with four non-centrosymmetric molecules: C_1. There are four molecules on the general position per unit cell. The present result is similar to the simulation, but obviously different in molecular symmetry and lattice parameters. The main cause for the disagreement is that MacLean and others assumed the molecular symmetry to be C_i, not C_1. Therefore, our lattice a is twice as long as the simulated one.

Figures 2(a) and 2(b) show the ORTEP plot of molecules A and B of the α form characterized by C_1 and C_i symmetry, respectively. In molecule A, the phenyl rings are deviated, in the same direction, from the heterocyclic system by 26.1° and 42.3°. Likewise, the t-BOC groups attached to the N atom of the heterocyclic ring are also twisted in the same direction by 46.0° and 40.0°. Furthermore, the heterocyclic ring system is not entirely planar, but is folded in the middle with a dihedral angle of about 179.7°. On the other hand, the heterocyclic system is entirely planar because of the C_i symmetry. The phenyl rings are also symmetrically twisted in the same direction by 25.3° and the torsion angle of the t-BOC group is 55.3°. The molecules of both conformations are stacked along the c-axis in the sequence of A-A-B-A-A-B- in a "herringbone" fashion as shown in Fig. 3.

Figure 4 shows the ORTEP plot of the molecule in the β form characterized by C_1 symmetry. The phenyl rings are asymmetrically deviated, in opposite directions, from the heterocyclic system by 34.3° and 29.3°. Similarly, the t-BOC groups are also asymmetrically twisted in opposite directions by 45.3° and 41.5°. Furthermore, the heterocyclic ring system is not entirely planar, but is folded in the middle with a dihedral angle of about 169.5°. The molecules are stacked along the a-axis relative to each other in a parallel arrangement as shown in Fig. 5.

TGA Measurements

Figures 6(a) and (b) show the TGA curves for the α and β forms. The weight loss begins to occur around 140°C, and ca 40% of the weight is lost around 200°C

TABLE I. Crystallographic Parameters for the α and β Forms of t-BOC DPP.

	α-form		β-form	
	This work[8]	Simulation[6]	This work[7]	Simulation[6]
Formula	$C_{30}H_{32}N_2O_6$	$C_{30}H_{32}N_2O_6$	$C_{30}H_{32}N_2O_6$	$C_{30}H_{32}N_2O_6$
Molecular weight	516.59	516.59	516.59	516.59
Crystal system	monoclinic	monoclinic	monoclinic	monoclinic
Space group	$P2_1/n$	$P2_1/n$	$P2_1/c$	$P2_1/c$
Molecular symmetry	C_1 & C_i	C_1 & C_i	C_1	C_i
a (Å)	10.437(2)	10.4851(4)	12.798(2)	6.2280(5)
b (Å)	21.367(4)	21.4631(6)	10.466(1)	10.2981(2)
c (Å)	16.799(3)	17.1342(1)	19.215(3)	19.467(3)
β (°)	96.64	95.245(2)	108.10(1)	90.4605(8)
Z	6	6	4	2
R factor	0.071	0.077	0.058	0.079

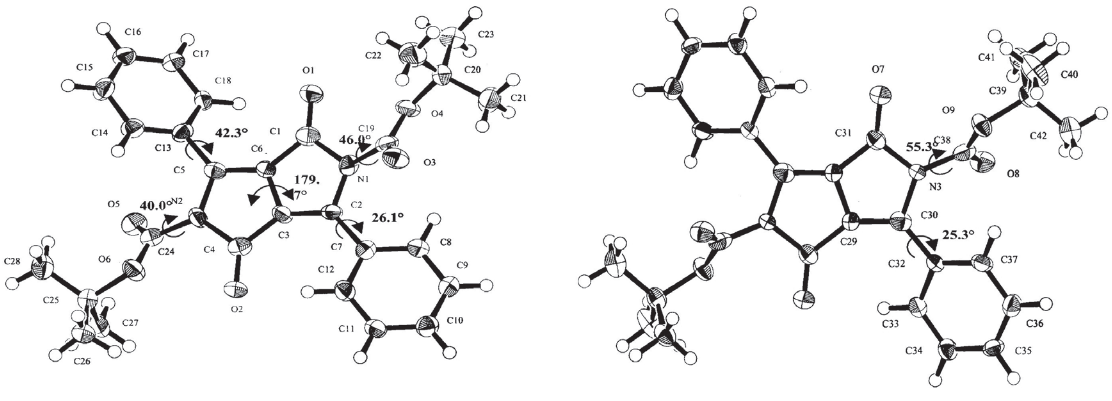

(a) (b)

Figure 2. ORTEP plot of molecules A and B for the α form: (a) molecule A and (b) molecule B.

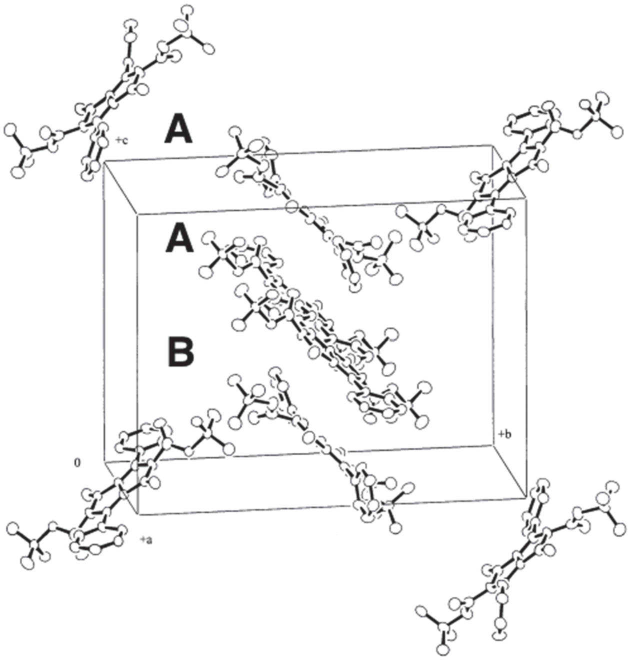

Figure 3. Molecular arrangement of the α form.

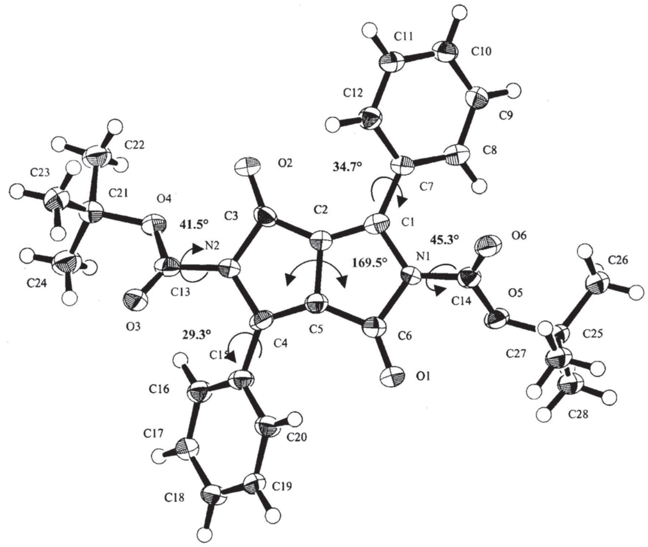

Figure 4. ORTEP plot of the molecule for the β form.

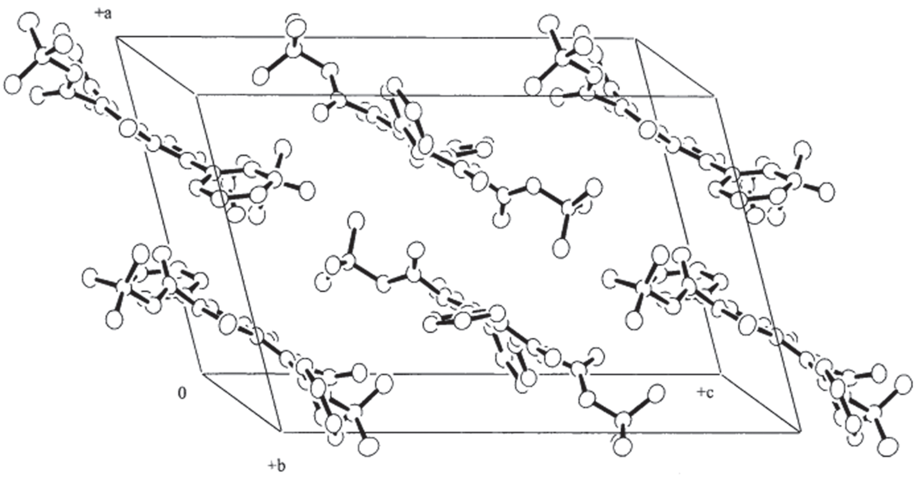

Figure 5. Molecular arrangement of the β form.

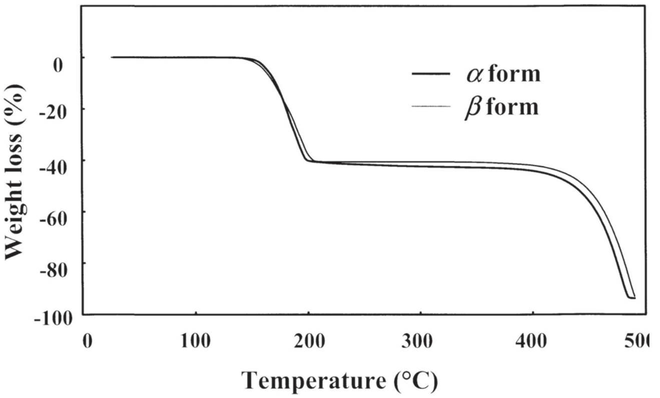

Figure 6. Thermogravimetric analysis on powdered substances for the α and β forms.

in both α and β forms, indicating the formation of DPP (*M*w: 488.54 in *t*-BOC DPP → 288.31 in DPP). During the decomposition process, *t*-BOC groups are completely eliminated and replaced by H atoms to form NH···O intermolecular hydrogen bonds between the NH group of one molecule and the O atom of the neighboring one. The color also changes from yellow to vivid red.

IR Spectra

Figure 7 shows the change of the IR spectra of *t*-BOC DPP monitored at various temperatures from 155 to 175°C during the regeneration process of *t*-BOC DPP. There are two C=O stretching bands around 1700 cm^{-1} at 155°C, one of which is due to the C=O stretching of *t*-BOC group and the other is assigned to the C=O stretching of the DPP skeleton. There are also observed two characteristic absorption bands of the methyl group around 1300 and 1100 cm^{-1}. The former is attributed to the vibrations due to the symmetry deformation while the latter is due to the rocking mode. Our focusing points during the regeneration process are the appearance of the NH stretching, displacement of the C=O stretching, appearance of NH···O hydrogen bond and disappearance of CH_3 vibrations. At 150°C where the weight loss begins to occur (Fig. 6), the C=O stretching bands remain around 1700 cm^{-1} and the two CH_3 bands are still observed. In addition, no NH stretching band is recognized around 3200 cm^{-1}. This indicates that the NH···O intermolecular hydrogen bond is not yet formed at this temperature. Then, the hydrogen-bonded NH stretching band begins to appear around 3200 cm^{-1} between 165 and 170°C. After that, the C=O stretching band is greatly displaced toward lower wavenumbers (around 1650 cm^{-1}) at 175°C. It is also to be noted that the two absorption bands resulting from the CH_3 group (deformation and rocking) have completely disappeared at this temperature. The NH and C=O stretching bands are considerably shifted toward lower wavenumbers. This is due to the stabilization of the NH and C=O stretching vibrations caused by the formation of NH···O hydrogen bonds. No further spectral change is recognized above 175°C.

Diffuse Reflectance Spectra

Figure 8 shows the diffuse reflectance spectra of the α and β forms measured on powders. The absorption peak around 500 nm in the α form makes the color slightly yellowish orange. Figure 9 shows the typical spectra at

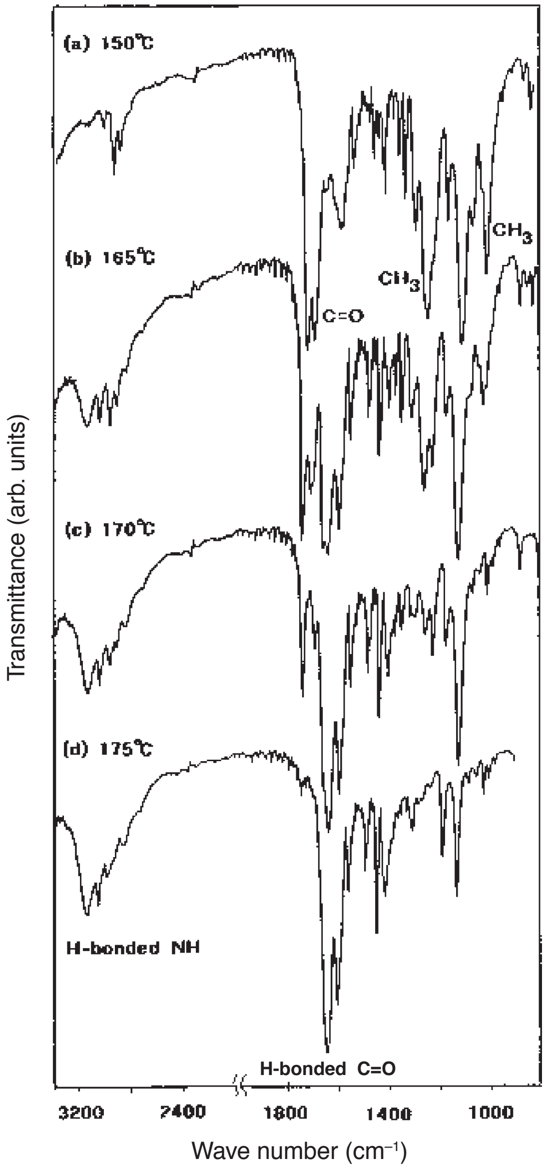

Figure 7. IR spectra of spin coated *t*-BOC DPP (β form) treated at various temperatures.

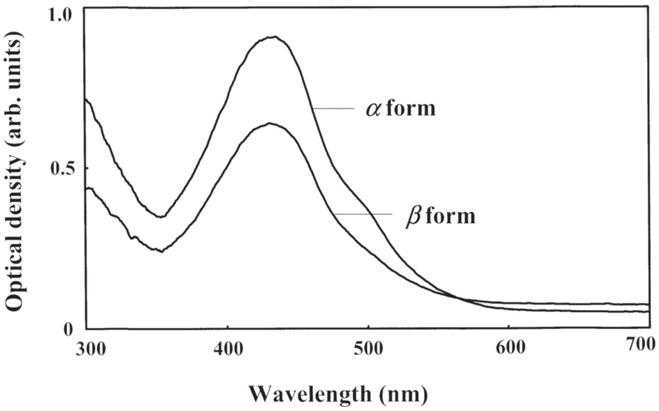

Figure 8. Diffuse reflectance spectra for the α and β forms.

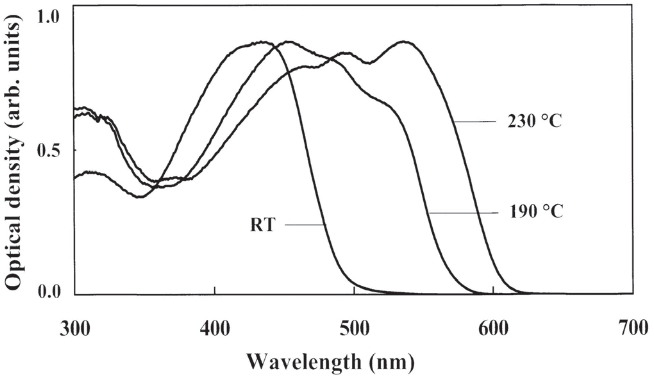

Figure 9. Diffuse reflectance spectra of *t*-BOC DPP (β form) treated at various temperatures.

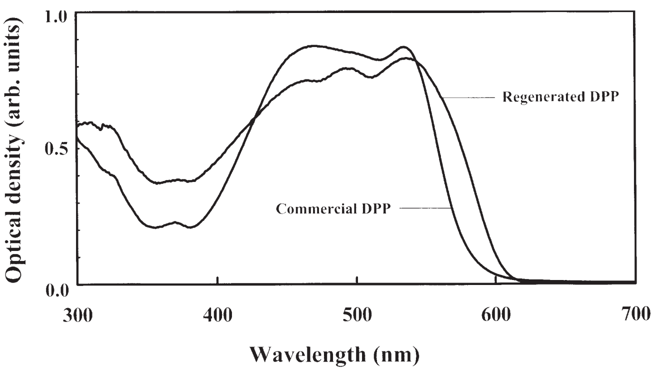

Figure 10. Comparison of the diffuse reflectance spectra: regenerated DPP and commercial DPP.

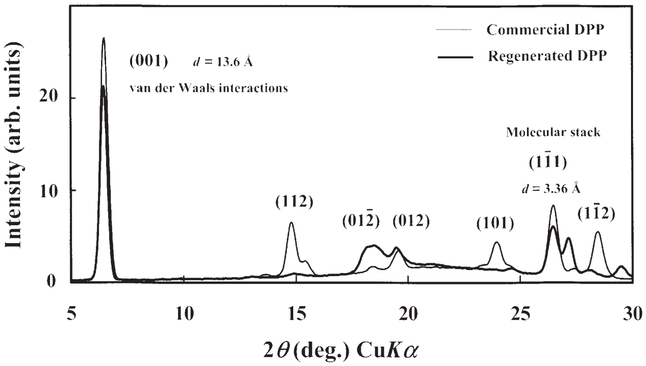

Figure 11. X-ray diffraction diagrams for both regenerated and commercial DPPs.

room temperature, 150 and 230°C in the process from *t*-BOC DPP (β form) to DPP. The color changes from yellow via yellowish red to vivid red. This means that the color varies as a function of temperature. In other words, it is quite difficult to fix a specified color in the intermediate state.

We will compare the diffuse reflectance spectrum of commercial DPP with that of regenerated DPP (Fig. 10). Apparently, the spectral shape as well as the absorption maxima is slightly different. Commercial DPP is more yellowish due to the absorption band around 460 nm. This indicates that the molecular arrangement in each product is slightly different as shown by the X-ray diffraction diagrams presented below.

X-Ray Diffraction Diagrams

Figure 11 shows the X-ray diffraction diagrams measured on powders for both commercial and regenerated DPPs. The diffraction peaks for commercial DPP is assigned on the basis of the structure analysis on single crystals.[5] The diffraction around $2\theta = 7°$ is assigned to the (001) plane, and the interplanar distance is about 13.5 Å. The (1–11) direction ($2\theta = 26.5°$) corresponds to the diffraction along the stacking axis (interplanar distance = 3.36 Å). The diffraction diagrams of these two samples are similar in low diffraction angles, although their intensities are slightly different. However, the diffraction diagrams are obviously different in higher angles, especially between 23 and 30° which include the diffraction along the stacking axis. This indicates that the phase of regenerated DPP is different from that of the commercial one, although the molecules are ar-

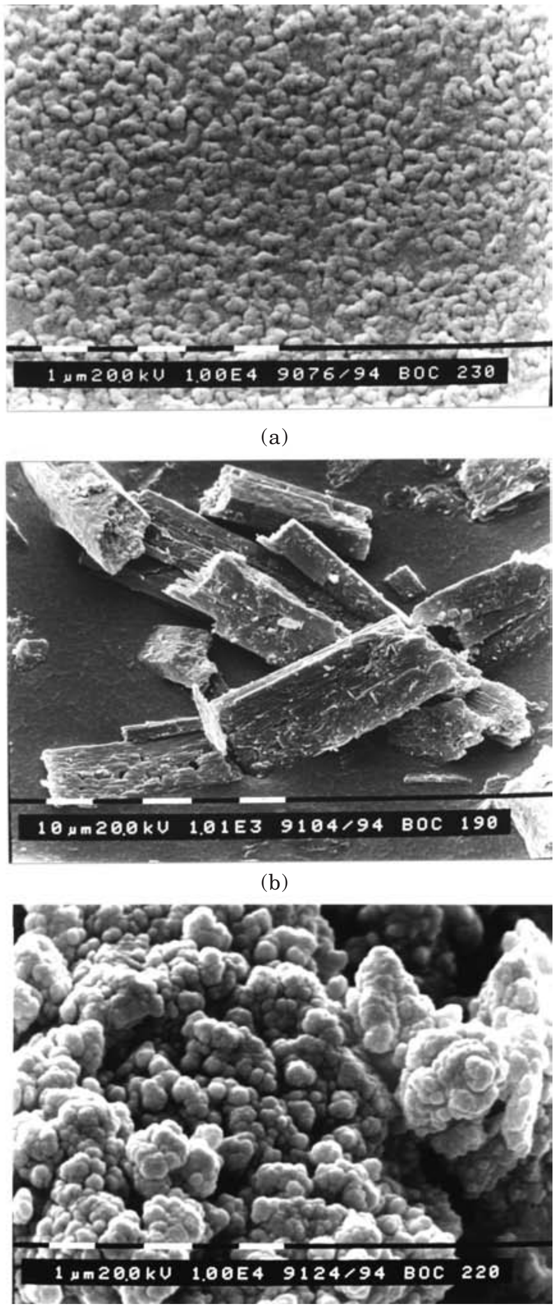

(a)

(b)

(c)

Figure 12. SEM pictures: (a) spin coated *t*-BOC DPP fired at 230°C, (b) *t*-BOC DPP powders fired at 190°C, and (c) *t*-BOC DPP powders fired at 220°C.

ranged, more or less, in the same way on the molecular plane due to the two-dimensional NH···O hydrogen bond network (Fig. 7). In addition, the phase of regenerated DPP is not so light and heat stable as that of the commercial product.

SEM Pictures of Regenerated DPP

Figures 12(a), 12(b) and 12(c) show the SEM (scanning electron microscope) photographs of the spin coated layers fired at 230°C, as well as regenerated powders fired at 190 and 220°C, respectively. In Fig. 12(a), a number of fine particles of the order of 0.2–0.3 μm are recognized in the form of islands. On the other hand, the regenerated samples in powders look quite different as shown in Fig. 12(b). We can see a number of square-rod crystals at the early stage of the firing around 190°C and then the formation of small particles at an elevated temperature of 220°C.

Conclusions

The crystal structure of *t*-BOC DPP as well as its transformation into the parent DPP have been studied in the present investigation. The conclusions are summarized as follows:

1. The crystal structure of the α form is in agreement with the simulated one, although the torsion angles are slightly different. The structure of the β form is similar to that of the simulation, but different in molecular symmetry and lattice parameters.
2. Transformation from *t*-BOC DPP to DPP begins around 160°C and is completed around 180°C.
3. A variety of colors appear during the regeneration process, accompanied by evolution of CO_2. Further color change occurs due to aging and dispersion in vehicles.
4. The color as well as the structure of regenerated DPP is slightly different from that of commercial one, and the heat and light stability is not as high as that of commercial product. ▲

References

1. W. Herbst and K. Hunger, *Industrial Organic Pigments*, VCH, Weinheim, Germany, 1997, p. 550.
2. J. Mizuguchi, Correlation between crystal and electronic structures in diketopyrrolopyrrole pigments as viewed from exciton coupling effects, *J. Phys. Chem. A* **104,** 1817 (2000).
3. J. Zambounis, Z. Hao and A. Iqbal, Pyrrolo[3,4-c]pyrroles, US Patent 5,484,943.
4. J. Zambounis, Z. Hao and A. Iqbal, Latent pigments activated by heat, *Nature* **388,** 131 (1997).
5. J. Mizuguchi, A. Grubenmann, G. Wooden, and G. Rihs, Structure of 3,6-diphenylpyrrolo[3,4-c]pyrrole-1,4-dione and 3,6-diphenyl-2,5-dimethylpyrrolo [3,4-c]pyrrole-1,4-dione, *Acta Cryst.* **B48,** 696 (1992).
6. E. J. MacLean, M. Tremayne, B. M. Kariuki, K. D. Harris, A. Iqbal, and Z. Hao, Structural understanding of a polymorphic system by structure solution and refinement from powder X-ray diffraction data: the α and β phases of the latent pigment DPP-BOC, *J. Chem. Soc., Perkin Trans.* **2,** 1513 (2000).
7. J. Mizuguchi, Refinement of the crystal structure of α-1,4-dioxo- 3,6-diphenylpyrrolo-[3,4-c]pyrrole-2,5(1H,4H)-dicarboxylic acid bis (1,1-dimethylethyl) ester, *Z. Krist. NCS.* **218,** 134 (2003).
8. J. Mizuguchi, The β-form of di-*tert*-butyl-1,4-dioxo-3,6-diphenyl-1,2,4,5-tetrahydropyrrolo[3,4-c]pyrrole-2,5-dicarboxylate, *Acta Cryst.* **E59,** 469 (2003).